

January 2008

A multiaxial stretchable interconnect using liquid-alloy-filled elastomeric microchannels

Kim Hyun-Joong

Son Chulwoo

B. Ziaie

Follow this and additional works at: <http://docs.lib.purdue.edu/ecepubs>

Hyun-Joong, Kim; Chulwoo, Son; and Ziaie, B., "A multiaxial stretchable interconnect using liquid-alloy-filled elastomeric microchannels" (2008). *Department of Electrical and Computer Engineering Faculty Publications*. Paper 49.
<http://dx.doi.org/http://dx.doi.org/10.1063/1.2829595>

This document has been made available through Purdue e-Pubs, a service of the Purdue University Libraries. Please contact epubs@purdue.edu for additional information.

A multiaxial stretchable interconnect using liquid-alloy-filled elastomeric microchannels

Hyun-Joong Kim,^{a)} Chulwoo Son, and Babak Ziaie^{b)}

School of Electrical and Computer Engineering, Purdue University, West Lafayette, Indiana 47907, USA

(Received 30 November 2007; accepted 4 December 2007; published online 3 January 2008)

We report on the fabrication and characterizations of a multiaxial stretchable interconnect using room-temperature liquid-alloy-filled elastomeric microchannels. Polydimethylsiloxane (PDMS) microchannels coated at the bottom with a gold wetting layer were used as the reservoirs which were subsequently filled by room-temperature liquid alloy using microfluidic injection technique. Using a diamond-shaped geometry to provide biaxial performance, a maximum stretchability of 100% was achieved ($\Delta R=0.24 \Omega$). Less than 0.02Ω resistance variation was measured for 180° bending. Active electronics, light emitting diode, was also integrated onto the PDMS substrate with stretchable interconnects to demonstrate stable electrical connection during stretching, bending, and twisting. © 2008 American Institute of Physics. [DOI: 10.1063/1.2829595]

Stretchable interconnects have recently attracted a considerable interest for flexible/conformal electronics such as displays, sensitive skin, and wearable electronics.¹⁻³ These applications require building active electronics/sensors on flexible substrates, which can deform into arbitrary shapes. This requires multiaxial stretchable (bendable and twistable) interconnects that can sustain large and repeated mechanical strain. Some recent efforts in this area include one-dimensional stretchable interconnects, flexible skin with two bending axes, and three-dimensional flexible metallic microstructures.⁴⁻⁷ However, these methods provide limited stretchability and employ complicated fabrication techniques. In our previous work, we presented two-dimensional (2D) diamond-shaped gold interconnect with liquid alloy joints on PDMS substrate.⁸ Even with over 60% stretchability, the previous design had low yield and a very limited bending capability due to the breakage of the gold lines. This paper reports on a design and fabrication method to overcome these weaknesses, increase the stretchability, and integrate surface mount active components.

Figure 1(a) shows a schematic view of a liquid-alloy-filled microchannel interconnect (straight-line structure). It consists of three PDMS layers including: (1) a microchannel embedded base layer, (2) a middle layer having inlet and outlet holes for microfluidic injection, and (3) a top capping layer. Figure 1(b) illustrates the fabrication process of the stretchable interconnect. SU-8 (SU-8 2100, MicroChem) mold on silicon wafers is prepared with 100 μm height through standard lithography process [Fig. 1(b)(i)]. Fresh PDMS (Sylgard 184, Dow coming, mixing ratio=10:1) is cast into the SU-8 mold (surface treated with trichlorosilane using desiccators for easy PDMS release from the mold) and then cured at room temperature for 48 h.⁹ After curing, PDMS is detached from the SU-8 mold, Fig. 1(b)(ii), followed by deposition of a gold wetting layer ($\sim 3000 \text{ \AA}$ thickness, e-beam evaporator) onto the substrate, Fig. 1(b)(iii). Gold layer on PDMS top surface is removed through repeated application of a sticky tape (3M, Scotch tape), while

leaving the gold layer at the bottom of microchannels intact [Fig. 1(b)(iv)].¹⁰

Middle PDMS layer having inlet and outlet holes for tubing is prepared separately and attached to the base PDMS layer, Fig. 1(b)(v). Surfaces of both PDMS layers are treated with O_2 -plasma (at 1.5 Torr pressure and 100 W power for 20 s) to increase adhesion followed by application of 90 °C on hotplate and pressure (by heavy weight) to bond the substrates.¹¹ The microchannel coated with thin gold layer on the bottom is then filled with room-temperature liquid-alloy (Indalloy60, Indium Corp., gallium/indium=75.5/24.5) by microfluidic injection technique, Fig. 1(b)(vi). The room-temperature liquid-alloy wets most metal films and the gold layer on the bottom of microchannel is used to improve the filling process.

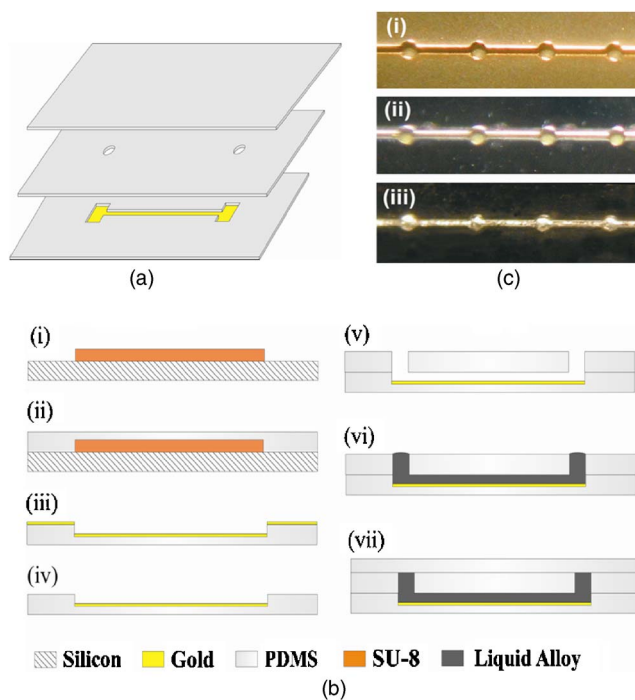


FIG. 1. (Color online) (a) Schematic view and (b) fabrication sequence of a straight-line stretchable interconnect, (c) optical images of (i) gold-coated PDMS surface, (ii) substrate after removal of the gold film from the top surface, and (iii) microchannel filled with liquid alloy.

^{a)}Electronic mail: kim116@purdue.edu. Tel.: 765-496-7594. FAX: 765-496-8299.

^{b)}Electronic mail: bziaie@purdue.edu.

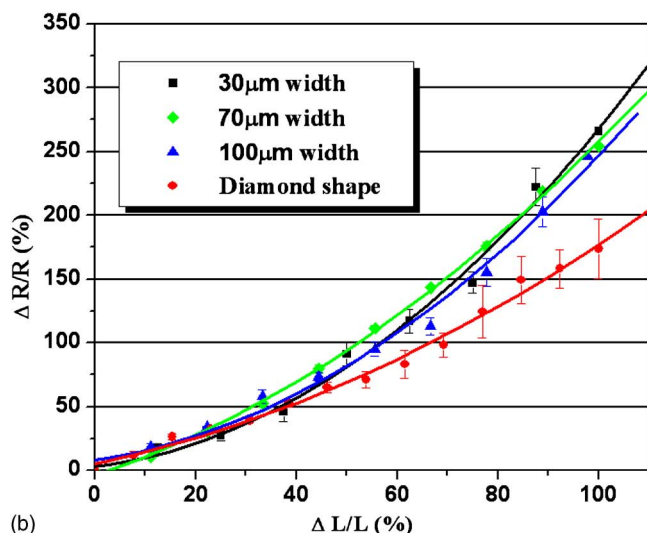
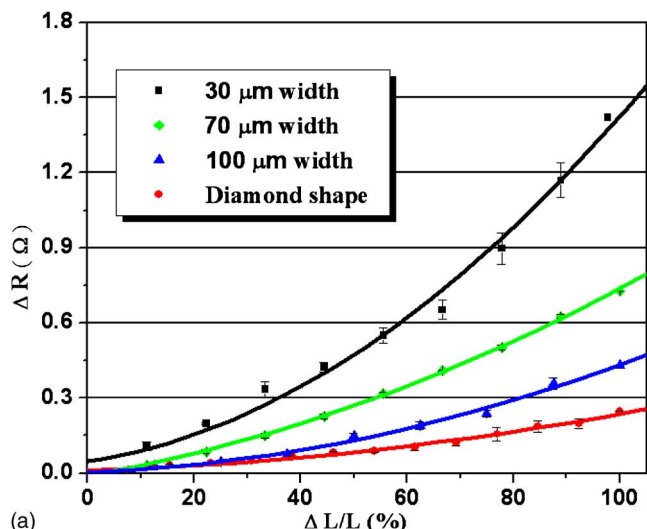


FIG. 2. (Color online) (a) Measured resistance variations (ΔR) vs strain (100 μm channel height) for straight lines having three different channel widths (30, 70, and 100 μm) and a 2D diamond shaped structure (100 μm width) and (b) relative resistance variations ($\Delta R/R$) vs strain.

To measure the resistance values, thin gold wires (37.5 μm diameter) are inserted into the liquid alloy reservoirs (at each end of interconnect) followed by capping the structure with the third PDMS layer (1 mm thick), Fig. 1(b)(vii). Fabricated interconnects are attached to two micropositioning stages (Newport 460A) on an optical table with mounting blocks placed on each end of the PDMS interconnect and tightening screws for stable clamping. Fixed interconnects are then stretched in one direction by a micro-manipulator. Four-point resistance measurement is performed to cancel out the resistance of the lead gold lines and contact resistance between the gold line and the liquid alloy reservoir. To measure the resistance variations, a constant current of ~ 30 mA is applied and the voltage variations are recorded by a high precision voltmeter ($\Delta R = \Delta V/I$) at an incremental length of 1 mm.

Figure 2(a) shows measured resistance variations (ΔR) versus strain ($\Delta L/L$). These include: (1) resistance of three different straight-line structures with the widths of 30, 70, and 100 μm , and (2) a 2D diamond-shaped interconnect (100 μm channel width). Both designs have a 100 μm channel thickness. The measured ΔR for each straight-line inter-

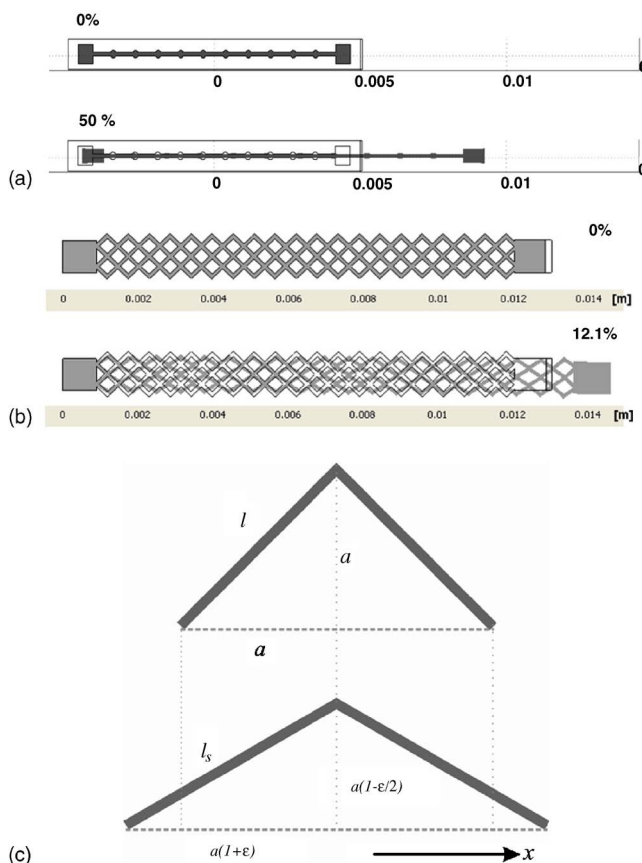


FIG. 3. (Color online) Illustration of microchannel deformations by strain for (a) a straight line and (b) a 2D diamond shaped. (c) Schematic view of a half unit cell in a diamond-shaped microchannel before and after stretching.

connect increases quadratically with the narrower lines showing a larger increase. The ΔR is the function of changes in length, width, and thickness of liquid alloy filled microchannels.

$$\Delta R = |R - R'| = \rho \left| \frac{L}{WT} - \frac{L'}{W'T'} \right|, \quad (1)$$

where ρ is the resistivity of room-temperature liquid alloy ($\sim 20 \mu\Omega \text{ cm}$). The length, width, and thickness of liquid alloy channels are L , W , and T , while L' , W' , and T' are the same parameters after the application of strain.

The length of the channel is increased by strain in the x direction ($L' > L$), while the width and thickness are both decreased ($W > W'$ and $T > T'$). At the same strain level, ΔR of the stretchable straight interconnect is therefore proportional to the width and thickness variations, i.e., $|1/WT - 1/W'T'|$. Assuming equal thickness variations at the same strain level, interconnects having a narrow channel widths show larger resistance change as compared to the ones having a wider channel width. Figure 2(b) shows measured relative resistance variations ($\Delta R/R$) versus strain ($\Delta L/L$). Measured $\Delta R/R$ of all straight-line structures has the almost same variations. This is due to the fact that the initial resistance value (R_0) of a channel with a narrower width is larger than that of a wider one resulting in a similar $\Delta R/R$ ratio for all three different designs.

As shown in Fig. 2, the diamond-shaped interconnect shows smaller variations (both absolute and relative) as compared to the straight-line ones. This is a result of the structural advantage of the diamond-shaped interconnect and can

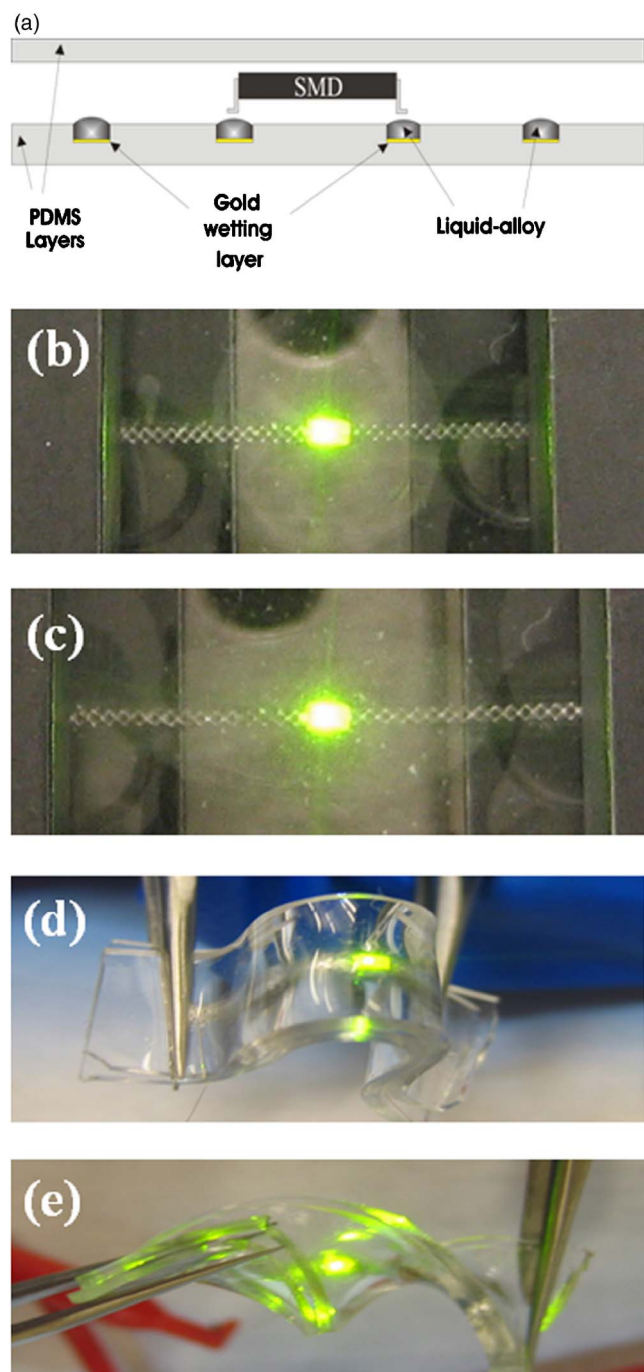


FIG. 4. (Color online) (a) Cross section of a surface mount active component integrated onto a stretchable interconnect and optical images of an LED (b) before and (c) after stretching, (d) bending, and (e) twisting the substrate.

be easily explained using a simple geometrical argument. Figures 3(a) and 3(b) illustrate the two-dimensional channel deformations of the straight-line and diamond-shaped interconnect subjected to a one-directional stretch. In the case of the straight-line structure, the length of the channel (current path) increases linearly with strain, however, for the diamond-shaped structure, the channel length does not change much resulting in smaller resistance variations. Figure 3(c) illustrates a schematic view of a half unit cell in a diamond-shaped microchannel before and after stretching. For simplicity, we assume that the unstretched unit cell is square shaped (equilateral right triangle quarter cell). One can show that the stretched channel length can be described

as follows, assuming a Poisson's ratio of 0.5 for PDMS.

$$l_s = \frac{l}{\sqrt{2}} \sqrt{(1 + \varepsilon)^2 + \left(1 - \frac{\varepsilon}{2}\right)^2}, \quad (2)$$

where ε is the strain in the x direction, l is the channel length segment before stretching, and l_s is the channel length segment after stretching. Using Eq. (2) for a strain of 50%, the diamond-shaped interconnects shows only 18.6% variation in the channel length, whereas the same strain results in 50% change for the straight lines.

Active electronic integration using surface mount devices (SMDs) can be accommodated by providing reservoirs for insertion of SMD legs. Although the components themselves are not stretchable, they can sustain a large deformation without being disconnected or dislodged by appropriate design of the reservoirs. Figure 4(a) shows a cross section schematic of a SMD active component integrated with stretchable interconnects. For PDMS substrates with active components, a lower stretchability of $\sim 30\%$ is measured (although releasing the strain results in the legs snapping back into the reservoirs, hence reconnecting the circuit). This is due to the constraint imposed by the limited size of the reservoirs allocated for the SMD legs. If a larger stretchability for active platforms is required, a bigger reservoir for SMD legs can provide such a capability. As a demonstration, an LED is integrated onto the substrate and stretched for up to 30%. Figure 4 shows the LED (Rohm Co., Ltd., SML-412MW) before (b) and after (c) stretching the substrate. Figures 4(d) and 4(e) demonstrate stable electrical connection during 180° bending and twisting each. The measured ΔR upon bending (up to 180°) is less than 0.02Ω for straight-line structure interconnects.

In conclusion, we designed and fabricated a multiaxial stretchable interconnect and characterized its performance. Maximum achieved stretchability ($\Delta L/L$) of a biaxial diamond-shaped interconnect was 100% with a 0.24Ω resistance variation (ΔR). The stretchability limit was due to the tearing of the PDMS substrate, which happened before any electrical disconnection. An active surface mount component was also integrate onto the substrate and was subjected to stretching, bending, and twisting without failure.

¹G. P. Crawford, *Flexible Flat Panel Displays* (Wiley, West Sussex, England, 2005).

²V. J. Lumelsky, M. S. Shur, and S. Wagner, *IEEE Sens. J.* **1**, 41 (2001).

³T. Martin, M. Jones, J. Edmison, and R. Shenoy, *Proceedings of the IEEE International Symposium on Wearable Computers*, 2003 (unpublished), p. 190.

⁴S. Wagner, S. P. Lacour, J. Jones, P.-H. I. Hsu, J. C. Sturm, T. Li, and Z. Suo, *Physica E (Amsterdam)* **25**, 326 (2004).

⁵D. S. Gray, J. Tien, and C. S. Chen, *Adv. Mater. (Weinheim, Ger.)* **16**, 393 (2004).

⁶N. Chen, J. Engel, S. Pandya, and C. Liu, *Proceedings of IEEE-MEMS Conference*, 2006 (unpublished), p. 330.

⁷A. C. Siegel, D. A. Bruzewicz, D. B. Weibel, and G. M. Whitesides, *Adv. Mater. (Weinheim, Ger.)* **19**, 727 (2007).

⁸H.-J. Kim, M. Zhang, and B. Ziaie, *Proceedings of IEEE-Transducers Conference*, 2007 (unpublished), p. 1597.

⁹K. W. Roh, K. Lim, H. Kim, and J. H. Hahn, *Electrophoresis* **23**, 1129 (2002).

¹⁰H. Schmid, H. Wolf, R. Allenspach, H. Riel, S. Karg, B. Michel, and E. Delamarche, *Adv. Funct. Mater.* **13**, 145 (2003).

¹¹Y. S. Shin, K. Cho, S. H. Lim, S. Chung, S.-J. Park, C. Chung, D.-C. Han, and J. K. Chang, *J. Microelectromech. Syst.* **13**, 768 (2003).